Available online at www.sciencedirect.com

ScienceDirect

Energy Procedia 158 (2019) 2780–2786

Energy Procedia

www.elsevier.com/locate/procedia

10th International Conference on Applied Energy (ICAE2018), 22-25 August 2018, Hong Kong, China

Additional Controls to Enhance the Active Power Management within Islanded Microgrids

Yuli Astriani[a,b], GM Shafiullah[a]*, Farhad Shahnia[a], Riza[b]

[a]*School of Engineering and Information Technology, Murdoch University, Perth, Australia*
[b]*National Laboratory for Energy Conversion Technology, Jakarta, Indonesia*

Abstract

Balancing the generated and consumed power in a microgrid is highly affected by the varying output power of the intermittent, renewable energy-based, distributed energy resources. This paper focuses on coordinating the output power among the energy resources within a microgrid while managing the consumed power at the demand side. The considered microgrid in this study consists of a battery system, which is the primary unit for grid-forming, as well as a photovoltaic system as the grid-following unit. A soft starting ramp function and an active power reduction function are implemented within the photovoltaic inverter respectively for the periods after the isolation of the microgrid from the grid and the over-frequency observation. Meanwhile, a demand-side management is developed based on the level of the battery's state of charge, to facilitate the microgrid with a longer time in supplying its critical loads.

Keywords: Islanded microgrid; load-shedding; over-frequency; power management; ; soft starting.

1. Introduction

Using renewable energies has become one of the attractive solutions worldwide to resolve greenhouse gas emission, as well as global warming, energy crisis, and energy cost, besides encouraging consumers to change their consumption behavior for conserving energy. However, high penetration of intermittent renewable energies may significantly affect the grid stability [1]. Assigning distributed energy resources (DERs) and the loads together in a limited area by forming a microgrid is expected to increase the grid reliability by more effectively managing the DERs and loads [2-3].

* Corresponding author. Tel.: +61-8-9360-6417; Fax: +61-8-9360-6346.
E-mail address: g.shafiullah@murdoch.edu.au

10.1016/j.egypro.2019.02.038

Microgrids are clusters of DERs and energy storages that can supply a group of local loads [4]. One of the advantages of microgrids is that they can operate in islanded mode to supply the load during planned or unplanned outages in the upstream utility feeder [5]. However, the intermittent output of renewable energy-based DERs makes microgrid's inertia smaller, because of the intermittency of renewable energies or using power electronic interfaces [6-7]. Another problem that may occur is the repeated connection/disconnection of a DER that tries to connect to the microgrid following over-voltage or over-frequency situations. Meanwhile, the use of large energy storage as has been limited due to its cost [8].

The most widely used controlling technique of a DER's output power within microgrids is the active power-frequency (P-f) droop control [9-10], as it uses the microgrid's frequency locally without any need for data communication amongst the DERs. On the other hand, a modified droop control is developed in [11] by implementing a derivative component in power-sharing control among the DERs, adding an adaptive neuro-fuzzy inference system in [12], and combining droop with an adaptive integral controller in [13]. A comprehensive review of droop control methods used in microgrids is presented in [14]. However, most of the proposed droop methods use the same droop gain for decreasing and increasing a DER's output power. Ref. [15] and [16] state that the value of the droop coefficient affects the speed of frequency restoration and the oscillations in the DER's output power. Therefore, in this study, a P-f droop control that has different coefficient s during ramping up and down of its output power is tested and analyzed. However, if the deviation between the generated and consumed power within the microgrid is large, an effective secondary frequency restoration is required [17].

The considered microgrid in this study consists of a battery system, which is the primary unit for grid-forming, as well as a photovoltaic system as the grid-following unit. A soft starting ramp method has been employed for grid-connected PV systems in [18] to mitigate the effects of sudden changes of solar irradiation or ambient temperature, and shows an enhancement versus the conventional maximum power point tracking algorithm. Therefore, a soft starting ramp is also implemented within the PV inverter for smoothing the starting sequence after the microgrid starts operating under islanded mode. Furthermore, a demand side management technique is also implemented for the microgrid to minimize the discharged energy from the battery so that the microgrid supplies the loads as long as possible under the islanded mode. To be able to perform demand-side management, microgrids often categorize their load as essential and non-essential [19]. Therefore, a simple sequence-based method has been implemented in this work for load-shedding, considering the battery's state of charge (SoC) level [20] so that microgrid can supply its essential loads as long as possible.

In summary, the main contributions of this study are to employ: (a) a P-f droop control approach to manage the output power of the renewable energy-based DERs; (b) a soft starting ramp for the DERs after the microgrid starts operating under islanded mode, and (c) a demand-side management to supply the essential loads longer. The proposed study will be useful in managing the active power adequately during islanded mode, preventing over-frequency, optimizing the utilization of renewable energies by avoiding their hard curtailment, and prolonging the supply period of essential loads.

2. Considered Microgrid Test Case and the Proposal

The considered microgrid in this study consists of a 10 kW PV array and inverter system, as well as a 10 kWh lithium battery, connected to a 380 volts three-phase microgrid, as shown in Fig. 1, and is located at the premises of the Agency for the Assessment and Research of Technology in Serpong, Indonesia. The battery's inverter provides bi-directional power flow while that of the PV is a grid-tied one. Some lighting and air conditioning loads are the assumed non-critical loads of the microgrid, and are subject to demand-side management.

When the microgrid disconnects from the grid and starts operating under the islanded mode, the battery's inverter shifts its operation mode from grid-connected to off-grid. This process takes 3 to 7 seconds. Meanwhile, the PV's inverter shuts down because there is no voltage and frequency reference in this period. Therefore, all loads will be unsupplied, except the essential ones. After a few seconds, the battery's inverter will form the grid and supply the loads, and consequently, the PV's inverter will start to operate under the grid-following mode.

According to the Indonesian grid code, in normal conditions, a DER must work at its nominal capacity in the frequency range of 49 to 51 Hz, whereas during disturbances, it is permitted to drop down to 47.5 Hz or rise up to 52 Hz [21]. Therefore, to comply with this standard, in this study, the operating frequency for battery inverter is considered from 47.5 to 51.5 Hz, while this figure is 47.5 to 51 Hz for the PV inverter. As the PV system is the secondary reserve during islanded operation, its maximal frequency is set lower than that for battery's inverter.

The islanding mode in this study is realized by disconnecting the microgrid from its upstream grid (i.e., by opening the switch at the point of common coupling). However, when the solar irradiation is high (e.g., during middays) but the load is low, the PV inverter start switching on and off repeatedly, as it tries to connect to the microgrid but fails because the microgrid frequency exceeds its allowed range. Therefore, a soft starting ramp and active power reduction function at over-frequency are employed in the PV inverter. Meanwhile, to prolong the islanding mode, the microgrid will shed the non-essential loads if the battery's SoC drops below a predefined level.

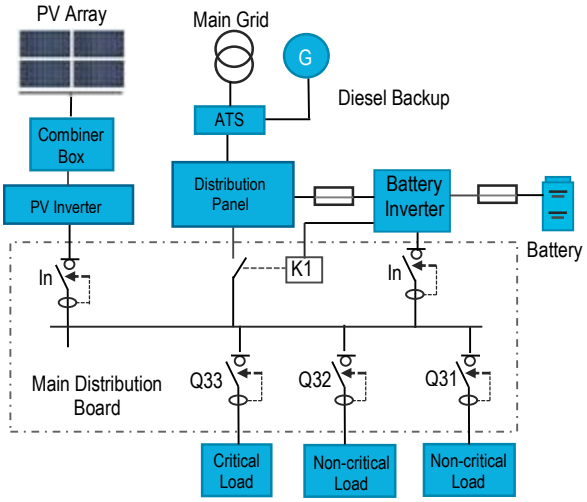

Fig. 1. Single-line diagram of the microgrid in the Agency for the Assessment and Research of Technology, Serpong, Indonesia.

2.1. Employing a soft starting ramp after microgrid isolation

During normal operation, the PV inverter is set to have an output power ramp-up of 10% (i.e., the output power of increases by 10% of its nominal value per second). The active output power (P) is a function of the current (I) following the maximum power point tracking algorithm. On the other hand, with a soft starting ramp function, two ramp-up gradients will affect the PV inverter output power, during the starting up after the isolation of the microgrid from the grid [22]. Thus, the output current of the PV inverter will be determined from

$$I_t = I_{t-1} + \left(k_{soft} \times k_{inc} \times I_{nom}\right) \tag{1}$$

in which I_t is the current at time t; I_{t-1} is the current at the previous time sample, and I_{nom} is the nominal current value while k_{soft} is the power gradient for starting up and k_{inc} is the gradient for increasing active power.

2.2. Employing an active power reduction at over-frequency

As microgrid is a localized power system, during islanded mode, the DERs output power must match with its load. Therefore, if the generated power is higher than the consumed power, the output power of the DER needs to be clipped. In this study, the function of the active power reduction uses a droop algorithm as

$$P_t = \begin{cases} P_{t-1} \times k_{Pdec} \times \left(f - f_{start}\right) & f \geq f_{start} \\ P_{t-1} + \left(P_{nom} \times k_{Pinc}\right) & f_{rst} \leq f \leq f_{start} \end{cases} \tag{2}$$

Thus, the PV inverter will inject all its output power to the microgrid as long as the frequency (f) is lower than the predefined starting frequency (f_{start}). When the frequency is higher than f_{start} , the droop controller will reduce the PV inverter's output power with a ramping slope of k_{Pdec}; however, when the frequency decreases to the resetting

frequency of f_{rst}, the PV inverter will increase its output power again by a defined gradient of k_{Pinc}. The values of f_{start} and f_{rst} are assumed higher than the nominal value to minimize the curtailment of PV, especially during grid-connected mode of the microgrid [23]. k_{Pdec} is set to 90% per Hz based on the ratio of the predicted output power of the PV system and the load capacity during the tests, while k_{Pinc} is 10% per second.

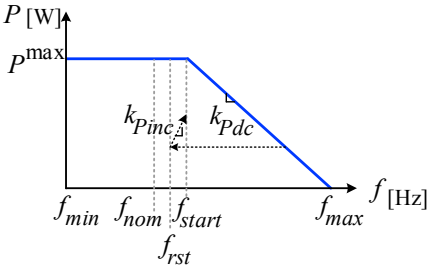

Fig. 2. Active power-frequency illustration control of PV inverter.

2.3. Employing an SoC-based load-shedding mechanism

The accurate information of a battery's SoC is important to determine its remaining capacity so that microgrid controller can predict how long the battery can supply its loads. Moreover, by monitoring the SoC's level, the battery's over-charge and over-drain can be avoided. Thus, its lifetime will be enhanced [24]. In the microgrid under consideration, the non-essential loads are divided into two groups:

- a group of lighting loads (through Q32 in Fig. 1) and considered as the least priority load, which will be disconnected when the battery's SoC reduces to 80%; and
- another group of lighting and air-conditioning loads (through Q31 in Fig. 1) and considered as the second least priority, which will be disconnected when the battery's SoC reduces to 50%.

3. Testing and Results

First, let us consider the microgrid of Fig. 1 in the grid-connected mode. During the testing, the average solar insolation was 841 W/m^2, and the module temperature was 49.5^{o}C. Therefore, the average predicted output power of PV system was calculated to be approximately 7.57 kW, based on the datasheet of the used PV module and inverter [25-27] while the total load was 1.5 kW. Fig. 3 shows that the output of the PV inverter along with the frequency.

Now, let us consider the microgrid under the islanded mode and before employing the new control mechanisms for the PV inverter. Fig. 4 shows that the microgrid's frequency increases alongside with the increment of PV output power. It takes around 4 seconds for the PV inverter to ramp up its output power from 0 to 3.6 kW as the default output power ramp up is 10% of its nominal capacity per second. When the PV inverter ramps up, subsequently the battery inverter ramps down its output power. As the operating frequency of PV inverter has been set in the range of 47.5 to 51 Hz, the PV inverter automatically shuts down when the microgrid's frequency reaches 51 Hz. After around 40 seconds, the PV inverter starts synchronizing again and tries to inject power. However, it shuts down again because of over-frequency.

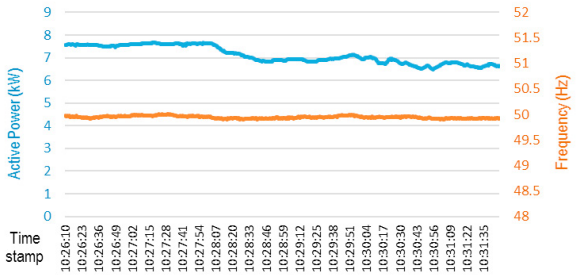

Fig. 3. Output power of the PV system in grid-connected mode, along with the system's frequency.

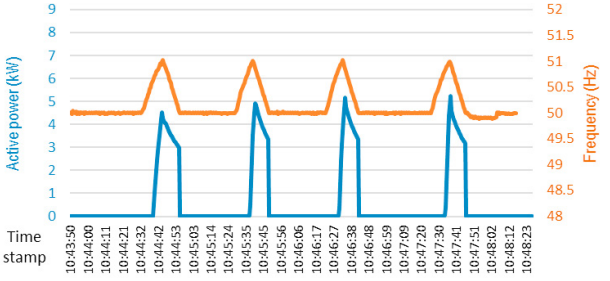

Fig. 4. Output power of the PV system under islanded mode, along with the microgrid's frequency.

Now let us consider the same microgrid after employing the proposed controllers. First, a power gradient of 1.2% is employed for soft starting ramp of PV inverter at the reconnection time, as well as a gradient of 20% for the active power increment. It can be seen from Fig. 5 that the slope of the active power increment or decrement is not as steep as the normal operation. Thus, it takes 80 seconds for the PV inverter to ramp up its output power from 0 to 2.5 kW. However, as the PV system's output power is much higher than the loads, it again shuts down before reaching its maximal output power due to over-frequency.

Fig. 4 and 5 show that the PV inverter shuts down when the microgrid's frequency reaches its maximum operating frequency. Therefore, it is needed to reduce the output active power of PV inverter so that microgrid runs in the allowed range of frequency. To this end, an active power reduction at over-frequency is implemented assuming f_{start} is 50.2 Hz while f_{rst} is 50.05 Hz while the above-mentioned soft starting ramp function is active. When the microgrid's frequency is higher than 50.2 Hz, the PV inverter reduces its output active power. As such, the frequency also decreases. When the frequency falls to 50.05 Hz, the PV inverter ramps up its active power again. It can be seen from Fig. 6 that after two risings and fallings, the system reaches its stable point at a frequency around 50.5 Hz while the PV inverter's output power is around 1.5 kW. Based on the testing result, it takes 7 minutes for the inverter to reach the desired value, which satisfies the 5-15 minute range specified in [28].

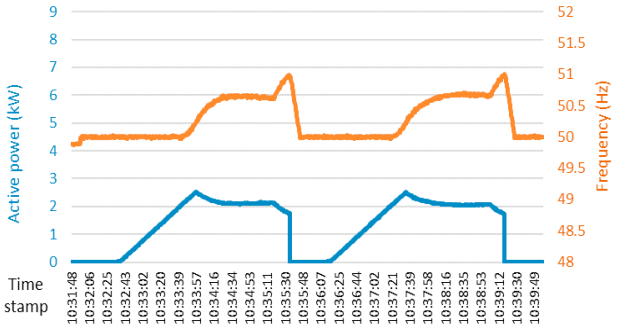

Fig. 5. Output power of PV system with the employed soft starting ramp after microgrid isolation.

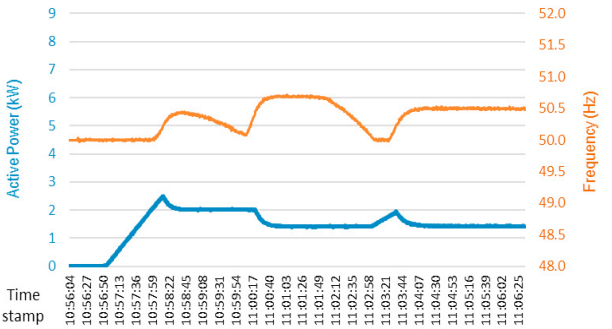

Fig. 6. Output power of PV system with the employed soft starting ramp and power reduction at over-frequency.

Another test is conducted assuming a predefined SoC level for switches Q31 and Q32 to disconnect their loads. The total load during the testing varies from 2.5 to 4 kW. Fig. 7 compares the battery's SoC with and without the implemented demand-side management. As seen from this figure, by implementing the demand-side management, switch Q32 opens at 0:43:16 when the battery's SoC drops to 80% while Q31 opens at 3:07:19 when the SoC drops to 50%. However, as seen from this figure, before applying this demand-side management, Q31 would have opened at 1:39:35. This shows that the microgrid with the implemented load-shedding can supply its essential loads longer.

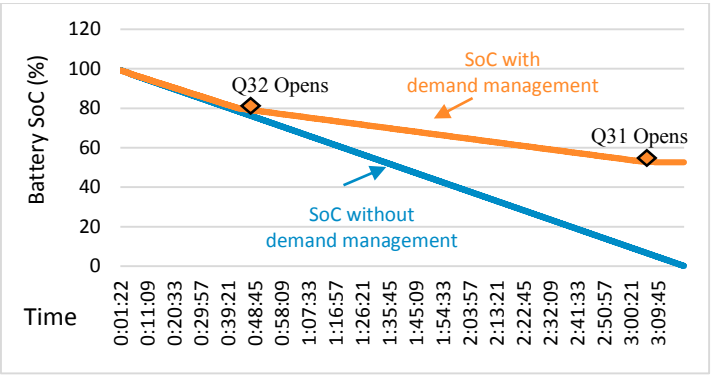

Fig. 7. Variations in the battery's SoC before and after implementing the SoC-based load-shedding of non-essential loads.

4. Conclusions

This paper has proposed and evaluated the impact of employing additional control mechanisms to the PV inverter of a microgrid operating under islanded mode to improve the active power management. Through practical measurements, it is shown that employing a soft starting ramp for the PV inverter can smooth the delivered power by the PV inverter when the microgrid starts operating under islanded mode. It is also demonstrated that disconnection of the PV inverter can be avoided at over-frequency situations by employing an active power reduction function for the PV inverter. The studies also verify that employing a demand-side management linked to the battery's SoC can prolong the power supply to the microgrid's essential loads.

It is planned to add an extra 90kWp PV array in this tested microgrid to test the microgrid's frequency and voltage performance with more diverse loads. Also, the demand response program will be in future advanced to consider the main grid's electricity spot price.

Acknowledgments

The authors would like to thank the Agency for Assessment and Research of Technology, Serpong, Indonesia, for the permit to perform testing and data retrieving of their microgrid system. The authors also thanks the Indonesian Ministry of Research, Technology and Higher Education for their financial support for this project.

References

[1] F. Shahnia, "Stability and eigenanalysis of a sustainable remote area microgrid with a transforming structure," *Sustainable Energy, Grids and Networks*, vol. 8, pp. 37-50, 2016.
[2] D.T. Ton and M.A. Smith, "The U.S. department of energy's microgrid initiative," The Electricity Journal, vol. 25, pp. 84-94, 2012.
[3] GM Shafiullah, "Hybrid renewable energy integration system for subtropical climate in Central Queensland, Australia", *Renewable Energy*, vol. 96, pp. 1034-1053, 2016.
[4] F. Shahnia, R.P.S. Chandrasena, S. Rajakaruna, and A. Ghosh, "Autonomous operation of multiple interconnected microgrids with self-healing capability," IEEE Power and Energy Society General Meeting, pp. 1-5, 2013.
[5] R.P.S. Chandrasena, *et al.*, "Control, operation and power sharing among parallel converter-interfaced DERs in a microgrid in the presence of unbalanced and harmonic loads, 23rd Australasian Universities Power Engineering Conference (AUPEC), pp. 1-6, 2013.
[6] MT Arif, AMT Oo, S Ali, GM Shafiullah, "Impacts of storage and solar photovoltaic on the distribution network", Proceedings in the 22nd Australasian Universities Power Engineering Conference (AUPEC), Bali, Indonesia, 2012.
[7] L.E. Luna Ramirez, T.S. Horacio and P.M. Fabio Andres, "Spinning reserve analysis in a microgrid," *Dyna*, vol.82, no. 192, pp. 85-93, 2015.
[8] K. Eger, *et al.*, "Microgrid functional architecture description", Siemens AG, Grenoble INP, Iberdrola S.A., Orange Labs, Synelixis Thales on FINSENY project, D3.3 v1.0, March 2013, pp.169
[9] Y.S. Kim, E.S. Kim, and S.I. Moon, "Distributed generation control method for active power sharing and self-frequency recovery in an islanded microgrid," *IEEE Trans. Power Systems*, vol. 32, pp. 544-551, 2017.
[10] R. Majumder, F. Shahnia, A. Ghosh, *et al.*, "Operation and control of a microgrid containing inertial and non-inertial micro sources," IEEE Region 10 Conference (Tencon), pp.1-6, 2009.
[11] S.J. Ahn, J.W. Park, I.Y. Chung, *et al.*, "Power-sharing method of multiple distributed generators considering control modes and configurations of a microgrid," *IEEE Trans. Power Delivery*, vol. 25, pp. 2007-2016, 2010.
[12] H. Bevrani and S. Shokoohi, "An Intelligent droop control for simultaneous voltage and frequency regulation in islanded microgrids," *IEEE Trans. Smart Grid*, vol. 4, pp. 1505-1513, 2013.
[13] J. Kim, J.M. Guerrero, P. Rodriguez, *et al.*, "Mode adaptive droop control with virtual output impedances for an inverter-based flexible ac microgrid," *IEEE Trans. Power Electronics,* vol. 26, pp. 689-701, 2011.
[14] U.B. Tayab, M.A.B. Roslan, L.J. Hwai, and M. Kashif, "A review of droop control techniques for microgrid," *Renewable and Sustainable Energy Reviews*, vol. 76, pp. 717-727, 2017.
[15] M. Chen and X. Xiao, "Hierarchical frequency control strategy of hybrid droop/VSG-based islanded microgrids," *Electric Power Systems Research,* vol. 155, pp. 131-143, 2018.
[16] Y.A.R.I. Mohamed and E.F. El-Saadany, "Adaptive decentralized droop controller to preserve power sharing stability of paralleled inverters in distributed generation microgrids," *IEEE Trans. Power Electronics,* vol. 23, pp. 2806-2816, 2008.
[17] R.P.S. Chandrasena, F. Shahnia, A. Ghosh, and S. Rajakaruna, "Secondary control in microgrids for dynamic power sharing and voltage/frequency adjustment," 24th Australasian Universities Power Engineering Conference (AUPEC), pp. 1-8, 2014.
[18] M. Balamurugan, S. K. Sahoo, and S. Sukchai, "Application of soft computing methods for grid connected PV system: A technological and status review," *Renewable and Sustainable Energy Reviews*, vol. 75, pp. 1493-1508, 2017.
[19] E Pashajavid, F Shahnia, A Ghosh, "Overload management of autonomous microgrids," IEEE 11th Int. Conf. on Power Electronics and Drive Systems (PEDS), Sydney, Australia, 2015.
[20] T. Hosseinimehr, A. Ghosh, and F. Shahnia, "Cooperative control of battery energy storage systems in microgrids," *International Journal of Electrical Power & Energy Systems*, vol. 87, pp. 109-120, 2017.
[21] Minister of Energy and Mineral Resources of Replubilic Indonesia. "The Regulation of Minister of Energy and Mineral Resources No. 3 Year 2007 regarding Jawa – Bali Grid Code", 2007, https://www.minerba.esdm.go.id/library/sijh/permen-esdm-03-2007.pdf

[22] SMA, “Sunny Tripower core1-US grid support utility interactive inverters”, http://files.sma.de/dl/29422/stp50-us-40-gridservices-ti-en-10.pdf
[23] SMA, “PV grid integration”, Technology Compendium 3.4, http://files.sma.de/dl/10040/pv-netzint-aen123016w.pdf
[24] J.P. Rivera-Barrera, N. Munoz-Galeano, and H.O. Sarmiento-Maldonado, “SoC estimation for lithium-ion batteries: Review and future challenges,” *Electronics*, 6, 102, 2017.
[25] Canadian Solar, “Quartech CS6P-260 | 265P”, datasheet, Sep. 2015, https://www.canadiansolar.com/downloads/datasheets/na/canadian_solar-datasheet-cs6pp_quartech-v5.3_na.pdf .
[26] SMA, “Sunny Tripower 5000TL – 12000TL”, datasheet, May 2017, http://files.sma.de/dl/17781/stp12000tl-den1723-v10web.pdf
[27] *How HOMER Calculates the PV Array Power Output*. https://www.homerenergy.com/support/docs/3.10/how_homer_calculates_the_pv_array_power_output.html
[28] T.L. Vandoorn, J.C. Vasquez, J. De Kooning, *et al.*, “Microgrids: Hierarchical control and an overview of the control and reserve management strategies,” *IEEE Industrial Electronics Magazine*, vol. 7, pp. 42-55, 2013.